On the origin of 140 GHz emission from the 4 July 2012 solar flare

Yuriy T. Tsap[a,b,*], Victoria V. Smirnova[b,c], Alexander S. Morgachev[b,d], Galina G. Motorina[b,e], Eduard P. Kontar[e], Valery G. Nagnibeda[c], Polina V. Strekalova[c]

[a] *Crimean Astrophysical Observatory, Nauchny, Crimea, 298409*
[b] *Pulkovo Observatory, Russian Academy of Sciences, Pulkovskoe Sh. 65, St. Petersburg, 196140, Russia*
[c] *Sobolev Astronomical Institute, Saint Petersburg State University, Universitetsky Pr.28, St.Petersburg, Petergof, 198504, Russia*
[d] *Radiophysical Research Institute, Nizhny Novgorod, Bolshaya Pecherskaya 25/12a, 603950, Russia*
[e] *School of Physics and Astronomy, University of Glasgow, Glasgow G12 8QQ, UK*

Abstract

The sub-THz event observed on the 4 July 2012 with the Bauman Moscow State Technical University Radio Telescope RT-7.5 at 93 and 140 GHz as well as Kislovodsk and Metsähovi radio telescopes, Radio Solar Telescope Network (RSTN), GOES, RHESSI, and SDO orbital stations is analyzed. The spectral flux between 93 and 140 GHz has been observed increasing with frequency. On the basis of the SDO/AIA data the differential emission measure has been calculated. It is shown that the thermal coronal plasma with the temperature above 0.5 MK cannot be responsible for the observed sub-THz flare emission. The non-thermal gyrosynchrotron mechanism can be responsible for the microwave emission near 10 GHz but the observed millimeter spectral characteristics are likely to be produced by the thermal bremsstrahlung emission from plasma with a temperature of about 0.1 MK.

*Corresponding author
Email addresses: yur_crao@mail.ru (Yuriy T. Tsap), vvsvid.smirnova@yandex.ru (Victoria V. Smirnova), a.s.morgachev@mail.ru (Alexander S. Morgachev), g.motorina@yandex.ru (Galina G. Motorina), eduard.kontar@glasgow.ac.uk (Eduard P. Kontar), vnagnibeda@gmail.com (Valery G. Nagnibeda), auriga-lynx@yandex.ru (Polina V. Strekalova)

Keywords: sub-THz solar flares; microwave and X-ray emissions; electron propagation

1. Introduction

Despite the unprecedented opportunities of modern terrestrial and cosmic telescopes, the detailed mechanisms of the solar flare energy release remain unknown. Therefore observations in poorly explored wavelength ranges can be very fruitful and important. Specifically, sub-THz observations corresponding to the frequency range of $10^2 - 10^3$ GHz *(*$3 - 0.3$ *mm)* can give us valuable information about the acceleration of electrons with energy $E \gtrsim 1$ MeV as well as the flare coronal and chromospheric thermal plasma (Raulin et al., 1999; Lüthi et al., 2004; Giménez de Castro et al., 2009; Fleishman & Kontar, 2010; Trottet et al., 2011; Krucker et al., 2013).

Solar sub-THz observations became available only in XXI century with Solar Submillimeter Telescope (Kaufmann et al., 2001) and Köln Observatory for Submillimeter and Millimeter Astronomy (Lüthi et al., 2004) in the $200 - 400$ GHz range. These first and subsequent observations of solar flares have shown that some events have a negative spectral slope, i.e., the spectral flux of radio emission decreases with frequency and can be considered as an extension of the gyrosynchrotron spectrum (Trottet et al., 2002; Raulin et al., 2004; Lüthi et al., 2004; Giménez de Castro et al., 2009). Surprisingly, other flares as a rule, long duration events, have revealed a positive spectral slope. This peculiarity can be observed during both the impulsive (Kaufmann et al., 2004; Silva et al., 2007; Kaufmann et al., 2009) and gradual (Trottet et al., 2002; Lüthi et al., 2004) flare phases. It should be emphasized that the observations mentioned above were obtained at frequency > 200 GHz and the frequency range of $100 - 200$ GHz has remained unavailable until recently. Meanwhile, the observations in this frequency range are important to improve the spectral coverage of the radio emission. We can suggest that the sub-THz events with the positive spectral slope at lower frequencies occur more often (see also Akabane et al., 1973; Correria et al., 1994; Chertok et al., 1995) and appropriate events are characterized by simpler magnetic configuration than long duration ones.

This work focuses on the analysis and interpretation of the 4 July 2012 flare. Special attention is paid to the sub-THz emission component observed at 93 and 140 GHz with the solar radio telescope RT-7.5 operated by the

Bauman Moscow State Technical University. Section 2 presents observations and instruments used in the study. Section 3 is dedicated to interpretations of obtained results. Section 4 presents discussion and main conclusions.

2. Instruments and observations

Sub-THz emission from GOES M5.3–class solar flare, which happened on 4 July 2012 in AR 1515 (S16W19), has been observed with the RT-7.5 solar radio telescope (Rozanov, 1981; Smirnova et al., 2013). This single-dish antenna of a Cassegrain-type with the diameter of 7.75 meters allows us to carry out simultaneous radio observations at two frequencies 93 and 140 GHz (3.2 and 2.2 mm). The half power beamwidths of the antenna are 1.5 and $2.5'$ at 140 and 93 GHz, respectively. Two super-heterodyne receivers are included into the quasi-optical scheme, i.e., beams are overlaped to observe one chosen area on the solar disk. The time constant of 1 s provides the sensitivity of the receivers of about 0.3 K.

Antenna temperatures are measured during observations relatively to the quiet-sun level. Experiments have shown that the contribution of noise of the receivers in the desired signal is about 1-1.5%. The maximum error of the beam pointing is $10''$ (Rozanov, 1981). In order to estimate the atmospheric attenuation of the signal from an active region the signals from the center of the solar disk and the sky are recorded at the same zenith angle when the absorption coefficient of the Earth's atmosphere did not change significantly. We estimated the observed quiet-sun temperatures by subtracting the sky temperature level. Then we compared these temperatures with the quiet-sun ones obtained from observations of the new Moon. As a result, the quit-sun temperatures turned out to be equal to 6600 and 6400 K at 93 and 140 GHz, respectively.

To provide the calibration of the flare flux densities we need the quite sun and sky brightness temperatures preferably near the beginning of solar burst. The observed quiet-sun and sky temperatures on 04 July 2012 were obtained about 8:30 UT. The atmospheric opacities for 93 GHz and 140 GHz at that time were equal to 0.1 and 0.25 Np, respectively. The corresponding uncertainties in the determination of the flare maximum flux densities were about 10 and 15%. We note that the sky was clear during the flare observations on 4 July 2012 but only the second flare burst (09:54:30-09:56:00 UT) was detected (Figure 1) because of the calibration map construction.

Microwave (centimeter) emission from the whole solar disk at 6.1 GHz frequency was obtained with the time constant of 1 s at Kislovodsk Mountain Astronomical Station. Observations carried out at a parabolic antenna with a diameter of 3 meters. Noise temperature of the antenna was about 1 K. Signal was detected by measuring of the antenna temperature. The conversion factors for solar fluxes units (sfu) derived from measurements of the moon temperature. Solar observations at 11.7 GHz (whole solar disk) were provided by the 1.8-m antenna located at Metsähovi Radio Observatory (Urpo, 1982). We also used measurements of total flux densities obtained by RSTN (San Vito) at 5.0, 8.8 and 15.4 GHz with the temporal resolution of about 1 s (Guidice et al., 1981).

Ultraviolet and X-ray diagnostics were done using SDO/AIA (Lemen et al., 2012), RHESSI (Lin et al., 2002), and GOES (White at el., 2005) instruments. These instruments are sensitive to the solar plasma in various temperature ranges: 0.5-20 MK (AIA), 4-40 MK (GOES), and above ~ 10 MK (RHESSI). RHESSI also allows observing hard X-ray emission in various energy bands. These spacecraft observations were complemented by H_α data from Kanzelhoehe Solar Observatory[1] with the imaging system providing 5 full-disk images per minute.

As shown in the panel [d] of Figure 1, the flux density at 140 GHz exceeds that of at 93 GHz and its maximum (09:55:30 UT) coincides with the maximum GOES light curves at 1-8 and 0.5-4 Å(panel [a]). The RHESSI light curves in ranges 25-50, 50-100, and 100-300 keV as well as microwave radio flux at 6.1, 8.8, and 11.7 GHz are presented in panels [b] and [c]. It is important to note that hard X-ray emission with photon energies > 50 keV is very weak and it has only one maximum as distinguished from the 25-50 keV time profile (panel [b] in Figure 1).

As it follows from the upper panel in Figure 2, the millimeter spectral index was, on average, equal to about 1.8 near the peak (09:55:24-09:55:36 UT) of emission. The error bars in our case indicate the error in measurements caused by the antenna and receiver noises, the beam pointing error as well as the atmospheric attenuation for millimeter emission. We note that the corresponding hard X-ray photon spectrum (Figure 2, lower panel) is characterized by the very steep slope. According to the spectrum-fitting procedure, a thermal part of the observed hard X-ray is fitted by the one-temperature plasma

[1]http://www.kso.ac.at

with emission measure $EM = 1.02 \times 10^{49}$ cm^{-3}, temperature $T = 2.3 \times 10^7$ K (1.95 keV)). In turn, the following parameters were used for a non-thermal part (thick target model): electron flux $F_e = 4.2 \times 10^{35}$ s^{-1}, spectral index $\delta_l = 7.3$, and low energy cutoff $E_l = 22.2$ keV.

The extreme ultraviolet (131 Å) and H_α images as well as RHESSI contours are presented in Figure 3. The RHESSI SSW IDL routines are used to provide the superposition of images. It can be seen that the location of the hard X-ray, ultraviolet, and H_α sources is not co-spatial. This suggests the important role of thermal processes during the flare energy release.

The differential emission measure (DEM)

$$\phi(T) = n_e^2 \frac{dl}{dT}, \tag{1}$$

where n_e is the electron number density, l is the distance along the line-of-sight, obtained from SDO/AIA data was constructed using regularization techniques (Kontar et al., 2005; Hannah & Kontar, 2012). Figure 4 suggests the DEM peak close to 13 MK but also demonstrate the presence of cooler coronal plasma.

3. Simulation and interpretation of millimeter emission

3.1. Thermal free-free emission

First of all, let us estimate the contribution of the thermal SDO plasma with broad temperature distribution ($10^{5.7} - 10^{7.3}$ K) into the free-free emission based on DEM (Figure 4).

The free-free absorption coefficient in the case of fully ionized plasma is (Dulk, 1985)

$$k_{ff} = \frac{K n_e^2}{T^{3/2} \nu^2},$$

where

$$K = 9.78 \times 10^{-3} \times \begin{cases} 18.2 + \ln T^{3/2} - \ln \nu, & T < 2 \times 10^5 \ K, \\ 24.5 + \ln T - \ln \nu, & T > 2 \times 10^5 \ K. \end{cases}$$

The optical depth $d\tau_\nu$ over distance dl can be written as

$$d\tau_\nu = k_{ff} dl = \frac{K n_e^2}{T^{3/2} \nu^2} dl, \tag{2}$$

where the electron density n_e and temperature T are functions of the distance along the line of sight l. According to equations (1) and (2) in the case of the optically thin source (e.g., Alissandrakis et al., 2013)

$$\tau_\nu = \int_{T_{min}}^{T_{max}} \frac{K\phi(T)}{T^{3/2}\nu^2} dT, \tag{3}$$

where T_{min} and T_{max} correspond to the temperature range of coronal plasma.

The brightness temperature of coronal plasma can be written in the form

$$T_b(\nu) = \int_0^\tau T e^{-\tau'_\nu} d\tau'_\nu,$$

and according to (1) and (2) we obtain the radio brightness temperature $T_b(\nu)$ related to the physical parameters of the flaring atmosphere

$$T_b(\nu) = \frac{1}{\nu^2} \int_{T_{min}}^{T_{max}} \frac{K\phi(T)}{\sqrt{T}} e^{-\tau_\nu(T)} dT. \tag{4}$$

In order to estimate the spectral flux density F_ν near the Earth, we use the Rayleigh-Jeans relation

$$F_\nu = \frac{2k_B\nu^2}{c^2} T_b(\nu) \frac{S}{R^2}, \tag{5}$$

where k_B is the Boltzmann constant, S is the projected area of radio source and R is the Sun-Earth distance.

The results of calculations on the basis of SDO/AIA imaging data and equations (3-5) have shown that the coronal SDO plasma with $T = 10^{5.7} - 10^{7.3}$ K cannot be responsible for sub-THz emission since the emission source becomes optically thick only at $\nu \lesssim 1$ GHz (Figure 5). Also it should give negligibly small contribution to centimeter emission from the 4 July 2012 flare *at* $S < 10^{18}$ cm^2. However, the SDO plasma can give significant but not decisive contribution to millimeter emission if the thermal source area $S > 10^{18}$ cm^2 (see also White & Kundu, 1992; Trottet et al., 2002, 2008, 2011).

Based on the obtained results and classification proposed by Reale (2014) we can suggest that millimeter emission is determined by the cool ($T \sim$ 0.1 MK) loops of the transition region. In order to estimate the contribution

of the appropriate plasma to the emission the well-known formula for the brightness temperature of the homogeneous plasma source

$$T_b(\nu) = T[1 - \exp(-\tau_\nu)], \tag{6}$$

as well as equations (2) and (5) can be used. As a result, for the total spectral flux we obtained

$$F_{total} = \frac{2k_B\nu^2}{c^2R^2}(T_{b1}(\nu)S_1 + T_{b2}(\nu)S_2), \tag{7}$$

where $T_{b1}(\nu)$ and $T_{b2}(\nu)$ are the brightness temperatures of sources associated with the cool and SDO plasma, respectively, S_1 and S_2 are the corresponding source areas.

The available data do not provide enough constraints to determine an unique set of parameters. As an illustration, this can be achieved for the following main parameters of the optically thick source which lead to the observed spectrum presented in Figure 6: area $S_1 = S_2 = 4 \times 10^{18}$ cm^2, geometrical depth $l = 10^9$ cm, plasma temperature $T = 0.1$ MK, and number density of thermal electrons $n_e = 7 \times 10^{10}$ cm^{-3}. The most interesting feature of proposed model is the large areas S_1 and S_2 and optical depth l of the optically thick cool source. The large scale ($\sim 60''$) thermal source with the temperature $T \sim 0.1$ MK was early proposed by Trottet et al. (2008) in order to explain a gradual, long-lasting (> 30 min) component of sub-THz emission from the energetic solar flare of 2003 October 28. In turn, the sufficiently large value of l implies the important role of cool loops in the generation of millimeter emission.

Let us now consider time profiles of flare emissions. As it follows from Figure 1 the maxima of sub-THz and soft X-ray emissions are coincident. This circumstance is in a good agreement with the assumption about the thermal origin of the sub-THz source. Meanwhile, the behavior of the hard X-ray and microwave time profiles is not the same. The hard X-ray time profile (25-50 keV) consists of two strong flare bursts with peaks at 09:54:30 and 09:55:00 UT, while the microwave and 50-100 keV profiles have only one near 09:55:00 UT (Figure 1).

The observed spectral flux of millimeter emission is quite weak and it does not exceed 40 sfu. Hence, in spite of the faint hard X-ray emission in the 100-300 keV (panel [b] in Figure 1) we can not exclude that the rising spectrum of sub-THz emission can be caused by the gyrosynchrotron emission of high

energy electrons in coronal loops (see also Bastian , 1999). Note that Razin suppression and free-free absorption which depend on the ambient plasma density should play an important role in the proposed model (e.g., Razin, 1960a; Razin, 1960b; Krucker et al., 2013).

The upper limit of the number density of high energy electrons n_h generated sub-THz emission in terms of hard X-ray observations can be estimated assuming that accelerated electrons responsible for gyrosynchrotron and hard X-ray emission represent the high energy (h) and low energy (l) parts of the common particle population. It is easy to show that number density of high energy electrons n_h with the lower energy $E_h \gtrsim 100\ keV$ does not strongly depends on its spectral index δ_h. Indeed, assuming the power-law spectrum of the low and high energy electrons in the energy ranges $[E_l, E_h]$ and $[E_h; \infty]$, respectively

$$n_{l,h}(E) = a_{l,h} E^{-\delta_{l,h}},$$

where $a_{l,h}$ are corresponding constants, excluding the jump in the point E_h, $n_l(E_h) = n_h(E_h)$, the relationship between the number densities of accelerated electrons at $(E_h/E_l)^{\delta_l - 1} \gg 1$ reduces to the form

$$n_h = \frac{\delta_l - 1}{\delta_h - 1} \left(\frac{E_l}{E_h} \right)^{\delta_l - 1} n_l \approx \left(\frac{E_l}{E_h} \right)^{\delta_l - 1} n_l. \quad (8)$$

Using the fit to the hard X-ray spectrum in Figure 2, assuming the hard X-ray source area $\approx 10^{17}$ cm^2 (50% contour in the RHESSI CLEAN 30-45 keV image) we get $n_l \sim 5 \times 10^9$ cm^{-3} and, in view of (8), $n_h \lesssim 4 \times 10^4$ cm^{-3}.Taking into account this restriction, we checked numerically the plausible parameter space based on the code proposed by Fleishman & Kuznetsov (2010) (see also Krucker et al., 2013) and found that we cannot easily reproduce the observed millimeter spectrum.

Thus, the bremsstrahlung mechanism of the thermal plasma with $T \approx 0.1$ MK can be responsible for the observed sub-THz emission from the 4 July 2012 solar event.

4. Discussion and conclusions

We have analyzed the sub-THz event observed on the 4 July 2012 with the RT-7.5 radio telescope at 93 and 140 GHz. It was revealed that the spectral flux of sub-THz emission increases with frequency between 93 and 140 GHz. It was concluded that the observed radio spectrum is well described

by the model, where sub-THz emission is due to the thermal bremsstrahlung mechanism. According to obtained estimates the emitting plasma with the temperature $T \approx 0.1$ MK occupied rather significant area $S \approx 4 \times 10^{18}$ cm^2 is required to explain the observed flux. Note that an important role of large low temperature thermal sources was early discussed by Lüthi et al. (2004) and Trottet et al. (2008, 2011) for other events.

The cosmic plasma with $T \approx 0.1$ MK plays a special role in the plasma astrophysics because energy losses caused by emission achieve the maximum at this temperature (Priest & Forbes, 2000; Colgan et al., 2008). Müller et al. (2003) have shown that the quite short (length $\lesssim 10$ Mm) loops with $T \lesssim 1$ MK can be cooled down quite rapidly due to the thermal instability caused by the plasma heating at the footpoints. In our view, this mechanism can be responsible for the increasing volume of the plasma with $T \sim 0.1$ MK during the flare energy release. The lack of observations with adequate temperature sensitivity and spatial resolution to observe plasma at 0.1 MK in the event studied prevents any firm conclusions. The role of relatively cool coronal loops needs to be investigated further to verify the thermal origin of 100-200 GHz emission. ALMA observations (Wedemeyer et al., 2015) can be very useful in this context.

We would like to thank the anonymous referees for very useful comments and detailed corrections, which we found to be very constructive and helpful to improve our manuscript. This work was particularly fulfilled within the framework of the Saint Petersburg State University Project No. 6.0.26.2010 and partially supported by the Programs of the Presidium of the Russian Academy of Sciences P-21 and P-22, the Russian Foundation for Basic Research (projects No.13-02-00277 A, 13-02-90472-ukr-f-a, 14-02-00924 A, and 16-32-00535-mol_a), the International Foundation of Technology and Investment (project No.01/00515) and the EU FP7 IRSES grant 295272 'RadioSun'.

References

Akabane, K., Nakajima, H., Ohki, K. et al., A flare-associated thermal burst in the mm-wave region, Solar Phys., 33, 431-437, 1973.

Alissandrakis, C.E., Kochanov, A.A., Patsourakos, S. et al., Microwave and EUV observations of an erupting filament and associated flare and coronal mass ejections, PASJ, 65, S8 (10 pp.), 2013.

Bastian, T.S., Impulsive flares: a microwave perspective, in Proceedings of the Nobeyama Symposium, held in Kiyosato, Japan, Oct. 2730, 1998, eds. T.S. Bastian, N. Gopalswamy, K. Shibasaki, NRO Report No.479., 211-222, 1999.

Chertok, I.M., Fomichev, V.V., Gorgutsa,R.V. et al. Solar radio bursts with a spectral flattening at millimeter wavelengths, Solar Phys., 160, 181-198, 1995.

Colgan, J., Abdallah, J.Jr., Sherrill, M. E. et al. Radiative losses of solar coronal plasmas, ApJ, 689, 585-592, 2008.

Correia, E., Kaufmann, P., & Magun, A., The observed spectrum of solar burst continuum emission in the submillimeter spectral range, in Proc. IAU Symp. 154, Infrared Solar Physics, eds. D.M. Rabin, J.T. Jefferies, C. Lindsey (Dordrecht: Kluwer Academic Publishers), 125-129, 1994.

Dulk, G.A. Radio emission from the sun and stars, Ann. Rev. Astron. Astrophys., 23, 169-224, 1985.

Fleishman, G.D., & Kontar E.P., Sub-Thz radiation mechanisms in solar flares, ApJ, 709, L127-L132, 2010.

Fleishman, G.D., & Kuznetsov, A.A. Fast gyrosynchrotron codes, ApJ, 721, 1127-1141, 2010.

Giménez de Castro, C.G., Trottet, G., Silva-Valio, A. et al., Submillimeter and X-ray observations of an X class flare, A&A, 507, 433-439, 2009.

Giménez de Castro, C. G., Cristiani, G. D., Simões, P. J. A. et al., A burst with double radio spectrum observed up to 212 GHz, Solar Phys., 284, 541-558, 2013.

Guidice, D. A., Cliver, E. W., Barron, W. R., et al., The Air Force RSTN System, In: Bulletin of the American Astronomical Society, 13, 553, 1981.

Hannah, I.G., & Kontar, E.P. Differential emission measures from the regularized inversion of Hinode and SDO data, A&A, 539, id.A146 (14 pp.), 2012.

Kaufmann, P., Raulin, J.-P., Correia, E. et al., Solar flare observations at submm-waves, in Proc. IAU Symp. 203, Recent Insights into the Physics of the Sun and Heliosphere: Highlights from SOHO and Other Space Missionsin, eds. P.Brekke, B.Fleck, J.B.Gurman (San Francisco: ASP), 283-286, 2001.

Kaufmann, P., Raulin, J.-P., Gimenez de Castro, C.G. et al., A new solar burst spectral component emitting only in the terahertz range, ApJ, 603, L121-L124, 2004.

Kaufmann, P., Trottet, G., Gimenez de Castro, C.G. et al., Sub-terahertz, microwaves and high energy emissions during the 6 December 2006 flare, at 18:40 UT, Solar Phys., 255, 131-142, 2009.

Kontar, E. P., Emslie, A. G., Piana, M. et al., Determination of electron flux spectra in a solar flare with an augmented regularization method: application to Rhessi data, Solar Phys., 226, 317-325, 2005.

Kontar, E.P., Bian, N.H., Emslie, A.G., & Vilmer, N., Turbulent pitch-angle scattering and diffusive transport of hard X-ray-producing electrons in flaring coronal loops, ApJ, 780, id.176 (10 pp.), 2014.

Krucker, S., Gimenez de Castro, C.G., Hudson, H.S. et al., Solar flares at submillimeter wavelengths, Astron. Astrophys. Rev., 21, id.58 (45 pp.), 2013.

Lemen, J.R., Title, A.M., Akin, D.J., et al., The atmospheric imaging assembly (AIA) on the solar dynamics observatory (SDO), Solar Phys., 275, 17-40, 2012.

Lin, R.P., Dennis, B.R., Hurford, G.J. et al., The Reuven Ramaty High-Energy Solar Spectroscopic Imager (RHESSI), Solar Phys., 210, 3-32, 2002.

Lüthi, T., Magun, A., & Miller, M., First observation of a solar X-class flare in the submillimeter range with KOSMA, A&A, 415, 1123-1132, 2004.

Müller, D.A.N., Hansteen, V.H., Peter, H., Dynamics of solar coronal loops. I.Condensation in cool loops and its effect on transition region lines, A&A, 411, 605-613, 2003.

Priest, E., & Forbes, T. Magnetic Reconnection: MHD Theory and Applications, Cambrige University Press, Cambrige, 2000.

Raulin, J.-P., White, S.M., Kundu, M.R. et al., Multiple components in the millimeter emission of a solar flare, ApJ, 547-558, 1999.

Raulin, J.P., Makhmutov, V.S., Kaufmann, P. et al., Analysis of the impulsive phase of a solar flare at submillimeter wavelengths, Solar Phys., 223, 181-199, 2004.

Razin, V.A., To the theory of radio emission spectra caused by discrete sources at frequencies lower than 30 MHz, Izv. Vyssh. Uchebn. Zaved., Radiofiz., 3, 584-594, 1960a.

Razin, V.A., On the spectrum of nonthermal cosmic radio emission, Izv. Vyssh. Uchebn. Zaved., Radiofiz., 3, 921-936, 1960b.

Reale, F., Coronal loops: observations and modeling of confined plasma, Living Rev. Solar Phys., 11, 4, 2014.

Reale, F., Landi, E., & Orlando, S. Post-flare ultraviolet light curves explained with thermal instability of loop plasma, ApJ., 746, id.18 (9 pp.), 2012.

Rozanov, B.A., Millimeter range radio telescope RT-7.5 BMSTU, in Reviews of USSR Universities, part 3, Radio electronics, 24, 3-10, 1981.

Silva, A.V.R., Share, G.H., Murphy, R.J. et al., Evidence that synchrotron emission from nonthermal electrons produces the increasing submillimeter spectral component in solar flares, Solar Phys., 245, 311-326, 2007.

Smirnova, V.V., Nagnibeda, V.G., Ryzhov, V.S. et al., Observations of subterahertz radiation of solar flares with an RT-7.5 radiotelescope, Geomagnetism & Aeronomy, 53, 997-999, 2013.

Trottet, G, Raulin, J., Kaufmann, P. et al., First detection of the impulsive and extended phases of a solar radio burst above 200 GHz, A&A, 381, 694-702, 2002.

Trottet, G., Krucker, S., Lüthi, T., & Magun, A., Radio submillimeter and γ-ray observations of the 2003 October 28 solar flare, ApJ, 678, 509-514, 2008.

Trottet, G., Raulin, J.-P., Giménez de Castro, G. et al., Origin of the submillimeter radio emission during the time-extended phase of a solar flare, Solar Phys., 273, 339-361, 2011.

Urpo, S. Observing methods for the millimeter wave radio telescope at the Metsähovi Radio Research Station and observations of the Sun and extragalactic sources, PhD thesis, Helsinki University of Technology, Espoo, Finland, 1982.

Wedemeyer,S., Bastian, T.. Brajsa, R. et al., Solar science with the Atacama Large Millimeter/submillimeter Array - A new view of our Sun, 2015, ArXiv e-prints.

White, S.M., & Kundu, M.R., Solar observations with a millimeter-wavelength array, Solar Phys., 141, 347-369, 1992.

White, S.M., Thomas, R.J., & Schwartz, R.A., Updated expressions for determining temperatures and emission measures from GOES soft X-ray measurements, Solar Phys. 227, 231-248, 2005.

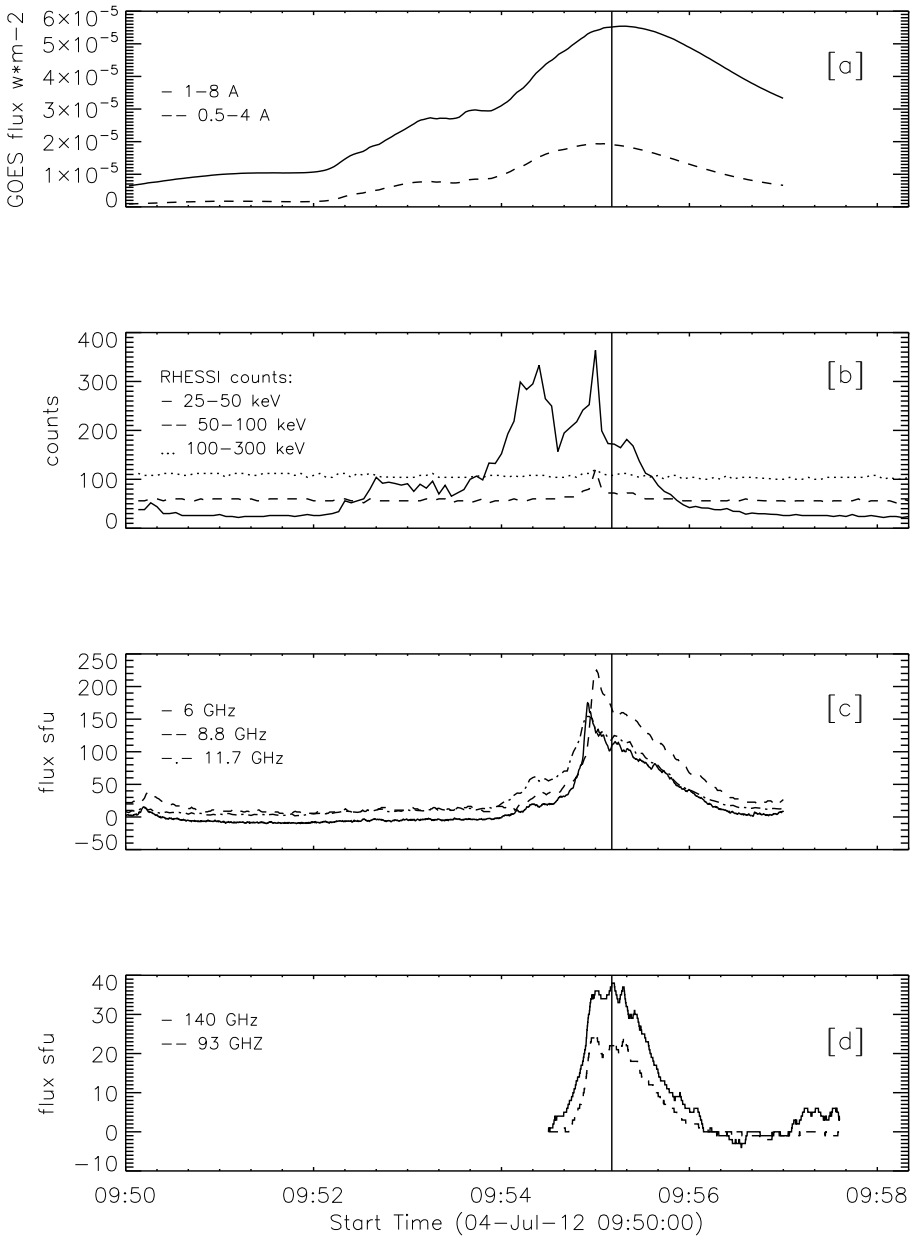

Figure 1: Light curves of soft X-ray [a], hard X-ray [b], microwave [c], and sub-THz [d] emissions from the 04 July 2012 solar flare obtained with GOES, RHESSI, Kislovodsk (6.1 GHz), Metsähovi (11.7 GHz), RSTN (San Vito, 8.8 GHz), and RT-7.5 (Bauman Moscow State Technical University) observations. The sub-THz emission maximum (09:55:09 UT) is marked by the perpendicular solid line.

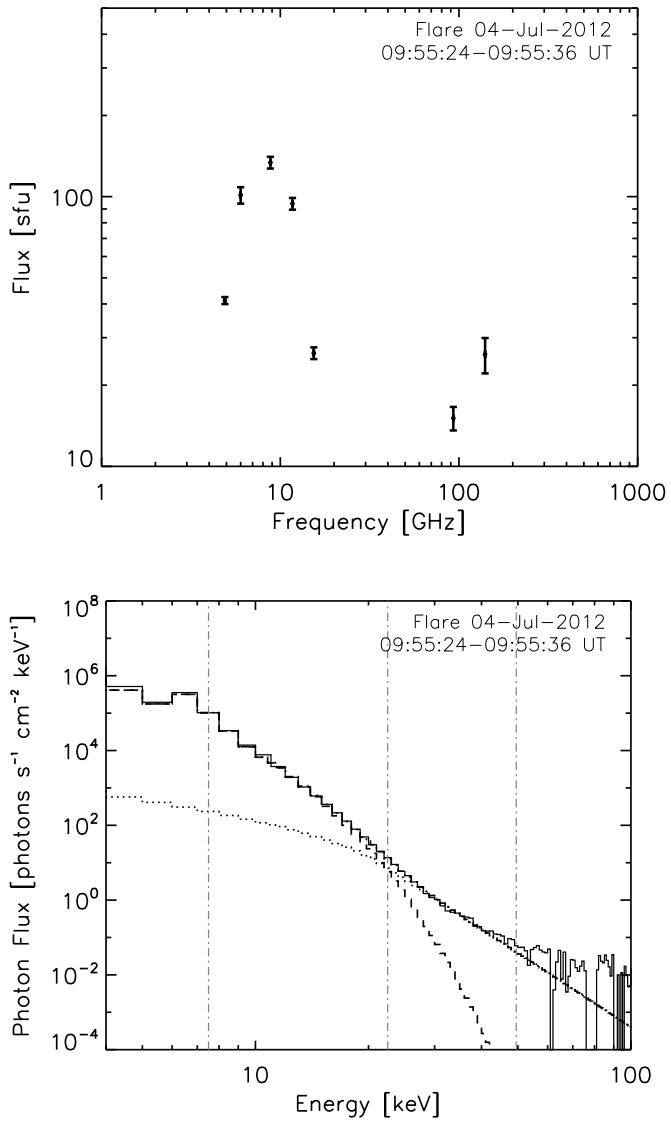

Figure 2: Upper panel: the averaged over the time interval (09:55:24-09:55:36 UT) radio flux density spectrum of the solar flare observed on 04.07.2012 at frequencies 6.1 GHz (Kislovodsk Mountain Astronomical Station), 11.7 GHz (Metsähovi solar radio telescope), 5.0, 8.8, and 15.4 GHz (RSTN, San Vito), 93 and 140 GHz (Bauman Moscow State Technical University). Lower panel: the *averaged* RHESSI X-ray spectrum (background subtracted data, solid line) fitted by the thermal (dashed line) and thick-target (doted line) models in the energy range from 7.5 to 49.5 keV. The summed fits of the spectra are shown by the dash-dotted line.

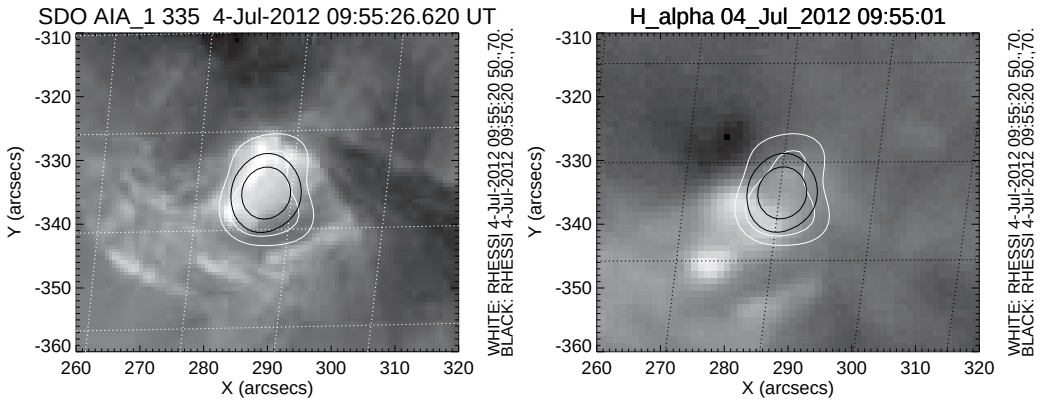

Figure 3: SDO/AIA (335 Å, left panel) and H_α (KSO, right panel) images. RHESSI contours (CLEAN algorithm) for the 7-10 and 30-45 keV channels (black and white lines, respectively) are shown at the 50 and 70% levels.

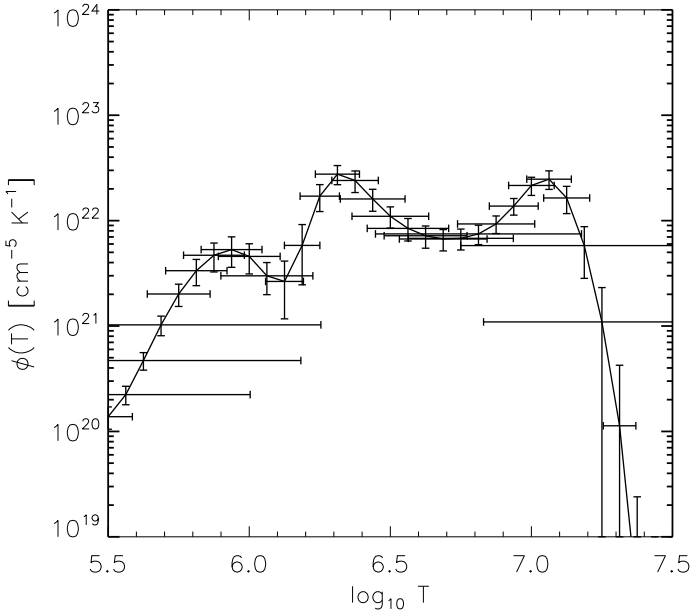

Figure 4: The differential emission measure $\phi(T)$ obtained based on SDO/AIA data for the 4 July 2012 solar flare (09:55:28 UT). The vertical and horizontal lines correspond to $\Delta\phi(T)$ and $\Delta \lg T$.

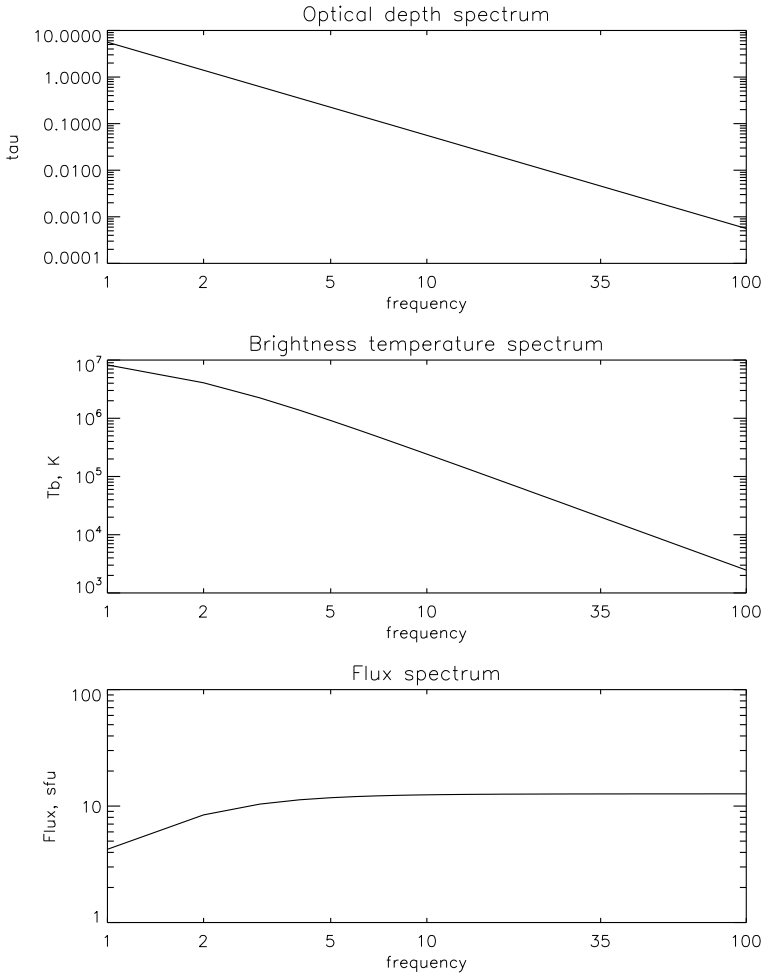

Figure 5: Numerical calculations of the thermal radio emission parameters on the basis of formulae (3-5) and the differential emission measure $\phi(T)$ (see Figure 4) obtained from SDO/AIA data. The spectral flux density is calculated for the source area $S = 10^{18}$ cm^2.

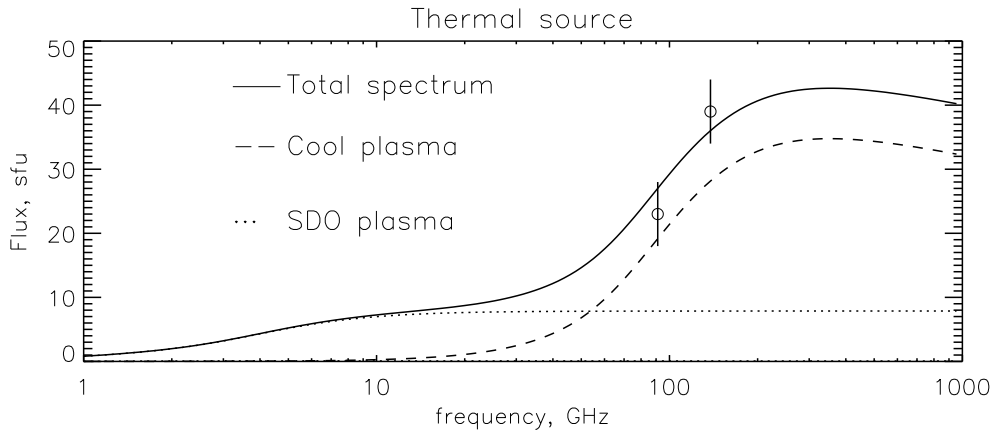

Figure 6: Results of numerical simulations of the free–free emissions from the 4 July 2012 solar flare (09:55:09 UT) based on equation (7).